

# Characterisation of human non-proliferative diabetic retinopathy using the fractal analysis

*Stefan Tălu<sup>1</sup>, Dan Mihai Călugăru<sup>2</sup>, Carmen Alina Lupascu<sup>3</sup>*

<sup>1</sup>Discipline of Descriptive Geometry and Engineering Graphics, Department of AET, Faculty of Mechanical Engineering, Technical University of Cluj-Napoca, Cluj-Napoca 400641, Romania

<sup>2</sup>Discipline of Ophthalmology, Department of Surgical Specialties and Medical Imaging, Faculty of Medicine, Iuliu Hatieganu University of Medicine and Pharmacy Cluj-Napoca, Cluj-Napoca 400012, Romania

<sup>3</sup>Department of Mathematics and Informatics, University of Palermo, Via Archirafi 34, Palermo 90123, Italy

**Correspondence to:** Stefan Tălu. Discipline of Descriptive Geometry and Engineering Graphics, Department of AET, Faculty of Mechanical Engineering, Technical University of Cluj-Napoca, 103-105 B-dul Muncii St., Cluj-Napoca 400641, Romania. stefan\_ta@yahoo.com

Received: 2014-06-01

Accepted: 2014-10-10

## Abstract

• **AIM:** To investigate and quantify changes in the branching patterns of the retina vascular network in diabetes using the fractal analysis method.

• **METHODS:** This was a clinic-based prospective study of 172 participants managed at the Ophthalmological Clinic of Cluj-Napoca, Romania, between January 2012 and December 2013. A set of 172 segmented and skeletonized human retinal images, corresponding to both normal (24 images) and pathological (148 images) states of the retina were examined. An automatic unsupervised method for retinal vessel segmentation was applied before fractal analysis. The fractal analyses of the retinal digital images were performed using the fractal analysis software ImageJ. Statistical analyses were performed for these groups using Microsoft Office Excel 2003 and GraphPad InStat software.

• **RESULTS:** It was found that subtle changes in the vascular network geometry of the human retina are influenced by diabetic retinopathy (DR) and can be estimated using the fractal geometry. The average of fractal dimensions  $D$  for the normal images (segmented and skeletonized versions) is slightly lower than the corresponding values of mild non-proliferative DR (NPDR) images (segmented and skeletonized versions). The average of fractal dimensions  $D$  for the normal images (segmented and skeletonized versions) is higher than the corresponding values of moderate NPDR images (segmented and skeletonized versions). The lowest

values were found for the corresponding values of severe NPDR images (segmented and skeletonized versions).

• **CONCLUSION:** The fractal analysis of fundus photographs may be used for a more complete understanding of the early and basic pathophysiological mechanisms of diabetes. The architecture of the retinal microvasculature in diabetes can be quantitative quantified by means of the fractal dimension. Microvascular abnormalities on retinal imaging may elucidate early mechanistic pathways for microvascular complications and distinguish patients with DR from healthy individuals.

• **KEYWORDS:** diabetic retinopathy; fractal; fractal dimension; retinal image analysis; retinal microvasculature

**DOI:10.3980/j.issn.2222-3959.2015.04.23**

Tălu S, Călugăru DM, Lupascu CA. Characterisation of human non-proliferative diabetic retinopathy using the fractal analysis. *Int J Ophthalmol* 2015;8(4):770-776

## INTRODUCTION

In the last few decades significant efforts have been directed to understand various aspects of the human retina using different computerized methods, for clinical diagnostics and treatment monitoring of retinal vascular diseases [1-5]. The retinal vascular imaging, as a noninvasive research tool, offers the potential to provide information for the detection, measurement, and quantifying of retinal vascular diseases.

Diabetic retinopathy (DR) is one of the most common microvascular complications of diabetes, characterized by gradually progressive alterations in the retinal microvasculature, and remains one of the leading causes of blindness worldwide [6-10].

Currently, the most commonly used classification of DR is a modified Airlie House/ETDRS (Early Treatment DR Study) classification that has been elaborated by the American Academy of Ophthalmology. Accordingly there describes three stages of non-proliferative DR (NPDR) with low risk of progression (pre-retinopathy; mild and moderate NPDRs), a stage of severe NPDR and a stage of proliferative DR (PDR). In NPDR the pathology remains intra-retinal while in PDR the pathology extends onto or beyond the retinal surface [11].

The most important risk factors for the development and progression of DR are disease duration, chronic hyperglycemia and systemic blood pressure levels. The mechanisms by which diabetes causes disease progression

and microvascular complications in the retina are not fully understood<sup>[6-10]</sup>.

DR transforms the morphology of retinal blood vessels (diameters, lengths, tortuosity, reflectivity, branch bifurcations, and angles) and the optimal density for capillary networks<sup>[6-8]</sup>. The changes in the retinal capillary walls develop gradually from the onset of diabetes mellitus and finally lead to capillary closure.

Parsons-Wingter *et al*<sup>[12]</sup> found that retinal vessel density varies with severity of DR. The vessel density of both arterial and venous trees oscillates with progression from mild NPDR to early PDR. It appeared to increase from mild to moderate NPDR, decrease from moderate to severe NPDR, and increase again from severe to very severe NPDR and early PDR. In spite of extensive ongoing research, the mechanisms and factors implied in the development of retinal vasculature are not fully understood owing to their extremely complicated and hierarchical structure<sup>[6-8,12-15]</sup>.

In ophthalmology, the fractal geometry offered both descriptive and predictive opportunities for the quantification of physical-chemical and biological phenomena over a range of spatial, temporal, and organizational scales<sup>[15-20]</sup>.

Structural retinal microvascular characteristics can be described using several methods based on the measurement of tortuosity, width, branching angle, branching coefficient, fractal dimension and of multifractal spectra<sup>[15,16]</sup>.

The three-dimensional human retinal microvascular network, as an observable circulatory system in the eye, can be analyzed and estimated if it is considered as fractal or multifractal object<sup>[13-17]</sup> in a "scaling window", which normally ranges in two to three orders of magnitude<sup>[18-22]</sup>.

The fractal concept offers a new dimension for analyzing the branching structure of retinal microvasculature. The fractal dimension  $D$  contains information about the global measure of complexity of the vascular branching pattern and is always a non-integer value that describes how irregular a fractal object is and how much of the space it occupies<sup>[13-18]</sup>.

In different fractal analysis studies of the normal human retinal microvascular network, the average values of the fractal dimensions were approximately 1.7<sup>[15,17]</sup>.

Investigators have also found different correlations between fractal dimension values associated with DR status, and their results are rather contradictory, apparently due to considerable variation in the experimental and methodological parameters involved<sup>[23-30]</sup>.

Avakian *et al*<sup>[23]</sup> found a significant difference between the fractal dimensions of vascular network of normal patients and patients with mild to moderate NPDR only in the macular region.

Lim *et al*<sup>[24]</sup> in the only prospective study to date, found no association between retinal fractal dimension with incident early DR in young patients with type 1 diabetes.

Cheung *et al*<sup>[25]</sup> found that greater retinal fractal dimension, representing increased geometric complexity of the retinal

vasculature, is independently associated with early diabetic retinopathy signs in type 1 diabetes. Also, fractal analysis of fundus photographs may allow quantitative measurement of early diabetic microvascular damage.

Kunicki *et al*<sup>[26]</sup> concluded that the box-counting and information fractal dimensions are not adequate parameters to be used in order to distinguish between normal and mild NPDR patients.

Grauslund *et al*<sup>[27]</sup> found that lower retinal fractal dimension was related to proliferative DR.

Cheung *et al*<sup>[28]</sup> showed that in the population-based study in older persons of mostly type 2 diabetes, no statistically significant associations between retinal fractal dimension with DR in individuals with diabetes.

Yau *et al*<sup>[29]</sup> concluded that there is no association between retinal fractal dimension and DR severity.

Nagaoka and Yoshida<sup>[30]</sup> found no association between fractal dimensions and any retinal circulatory parameters of the retinal arterioles. In contrast, they found significant correlations between the fractal dimensions and the retinal vessel diameter and the retinal blood flow in the retinal venules.

Multifractal analysis can be used to describe the progressive alterations in the human retinal microvasculature both locally and globally, being more sensitive in detection of retinal microvascular changes than the fractal analysis (a globally description over the retinal regions)<sup>[16,20,21,31]</sup>. The fractal and multifractal analyses of retinal vascular network depends on the algorithm and specific calculation used<sup>[32-36]</sup>. No multifractal analysis study of retinal microvascular network in DR eyes was found in the available ophthalmologic literature.

## SUBJECTS AND METHODS

**Fractal Analysis** Let's consider a fractal object recorded into a digital image. Let  $A$  be any nonempty bounded subset of  $R^n$  ( $n$ -dimensional Euclidean space  $R^n$ ). The fractal dimension gives the scaling between the smallest number of  $n$ -dimensional  $\varepsilon$  boxes needed to cover the set  $A$  completely, and the boxes' size  $\varepsilon$ . The fractal dimension based on the box-counting method ( $D_{BC}$ ) of  $A$  is defined with the following equation<sup>[37]</sup>:

$$D_{BC}(A) = \lim_{\varepsilon \rightarrow 0} \frac{\log N_{\varepsilon}(A)}{\log(1/\varepsilon)} \quad (1)$$

where  $N(\varepsilon)$  represents the number of non-empty boxes of size  $\varepsilon$  needed to cover the fractal structure. This method is computationally much faster than most other fractal estimation methods.

In equation (1) the zero limit cannot be applied to medical and biological images and  $D_{BC}(A)$  can be estimated by means of next equation:

$$D_{BC}(A) = D \quad (2)$$

where  $D$  is the slope of the regression line for the log-log

plot of the scanning box size and the count from a box counting scan. The "count" usually refers to the number of grid boxes that contained pixels in a box counting scan. The slope of the linear region of the plot is  $(-D)$ , where  $D$  is the box-counting dimension that corresponds to the fractal dimension.

**Segmentation Method** The segmentation consists of extracting geometric information about the retinal vessels from the eye fundus images. The color images were converted to grayscale. The segmented images were saved in tif format. In this study, an automatic unsupervised method for the segmentation of retinal vessels<sup>[38]</sup>, according the segmentation methodology and computer algorithms proposed in papers<sup>[39-41]</sup>, was applied before fractal analysis.

**Subjects** This study was conducted according to the recommendations of the Declaration of Helsinki for research in human subjects. The protocol was approved by the Ethics Committee of "Iuliu Hatieganu" University of Medicine and Pharmacy Cluj-Napoca, Romania. The patients, treated in the Ophthalmological Clinic in Cluj-Napoca, Romania, were enrolled after written informed consent.

Of 190 eligible participants, 172 participated in the study, conducted from 10<sup>th</sup> January, 2012 to 20<sup>th</sup> December, 2013. Of 172 participants, 164 subjects (95.3%) had fundus photographs taken of either eye and 8 had photographs from the right eyes available for retinal vascular analysis. We excluded eyes with poor image quality ( $n=8$ ) and with evidence of previous laser treatment ( $n=10$ ). This left 172 subjects for the final analysis (90.5% of 190 participants). All participants underwent a standardized interview and ocular and systemic examination.

Diabetes was defined as random plasma glucose of greater than or equal to 200 mg/dL (11.1 mmol/L), the use of diabetes medication, or physician-diagnosed diabetes. The results were expressed as mean $\pm$ standard deviation (SD).

The normal healthy subjects (group 1) consisted of 24 volunteers (male gender, 58.3%; age,  $52\pm 8.6$ y) with normal posterior pole and without ocular or systemic diseases.

Group 2 included 50 patients (male gender, 44.0%; age,  $54\pm 6.2$ y) with mild NPDR. Changes that have developed in these patients were mainly represented by microaneurysms, usually in the area temporal to the macula. At this stage macula edema with retinal thickening or lipidic hard exudate formation were encountered only in a few patients. Unless the macula was affected then NPDR had little effect on the visual acuity.

Group 3 encompassed 46 patients (male gender, 47.8%; age,  $51\pm 9.3$ y) with moderate NPDR. In addition to retinal microaneurysms, the clinical picture of these patients was represented by other features elsewhere in the fundus such as cotton wool spots, superficial flame shaped hemorrhages, or the more deeply placed blotch or cluster hemorrhages, venous dilatation, venous beading or loops, and intraretinal microvascular abnormalities (IRMA). All of these changes

were limited to two quadrants of the retina.

Group 4 included 52 patients (male gender, 48.0%; age,  $56\pm 5.9$ y) with severe NPDR. Intraretinal microvascular abnormalities (vascular bypasses), venous beading and severe amounts of blotch hemorrhages were presented in more than two quadrants of the retina; they were signs of retinal non-perfusion and ischemia in the absence of neovascularization and represented hallmarks of severe NPDR. There were extensive areas where capillary bed was closed (capillary non-perfusion zones), nerve fiber layer infarcts and severe macular edema.

The slides were captured by a fundus camera at 45° field of view (VISUCAM<sup>Lite</sup> Zeiss; Carl Zeiss Meditec AG 07740 Jena 2008, Germany) after pupil dilation using tropicamide 1% and phenylephrine hydrochloride 2.5%.

The technical data of VISUCAM<sup>Lite</sup> Zeiss are: capture one 1/2"CCD each for color and black-and-white; display 15" LCD monitor (1024  $\times$  768 pixels); field angle 45°; image mask 45°; types of image capture color; working distance 40 mm; patient's eye, front lens; focusing range  $\pm 25$  D, continuous; swivel range  $\pm 40^\circ$ , horizontal; operating system Windows XP professional; mainboard Zeiss embedded PC; Export Image formats: dcm, bmp, jpeg; VISUPAC archiving and image analysis system.

**Methods** Figures 1-4 show images of the retina vessel network for: a normal subject (Figure 1); a patient with mild NPDR (Figure 2), a patient with moderate NPDR (Figure 3) and a patient with severe NPDR (Figure 4).

Reproducibility of the measurements was high, with intra-grader and inter-grader intra-class correlation coefficients ranging from 0.972 to 0.985. The measurements were performed by 2 trained graders using a standardized grading program. The inter-grader and intra-grader reliability were computed using the kappa statistics. The intra-class correlation coefficient (ICC) value of 0.81-1.00 indicates almost perfect agreement.

The images were exported to Adobe Photoshop CS6 (Creative Suite 2, Adobe, San Jose, CA, USA), and to improve image quality by intensifying the vascular network while decreasing background noise in nearby regions, the unsharp mask filter with a radius of 10 pixels was applied. This tool sharpens the pixels in an image to make it substantially clearer. Finally, the images were processed in MATLAB software R2012b, MathWorks, Inc. The entire algorithm has been previously described in detail in Gould *et al*<sup>[42]</sup>.

The segmented version of retinal vessel structure contains the vessel silhouettes extracted from the fundus photographs.

The binary skeletal structure (8-bit) of retinal vessel structure was obtained by mathematical morphologic processing from the original micrograph images with one single pixel in width, but without any change in relative location and configuration of each element.

This procedure was applied for all analyzed structures. All

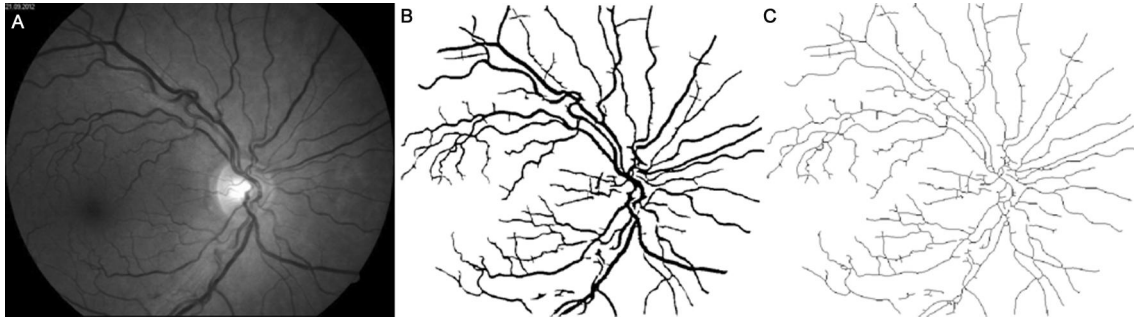


**Figure 1** Image of a normal state retinal vessel network A: The grey image version; B: The segmented version; C: The skeletonized version.

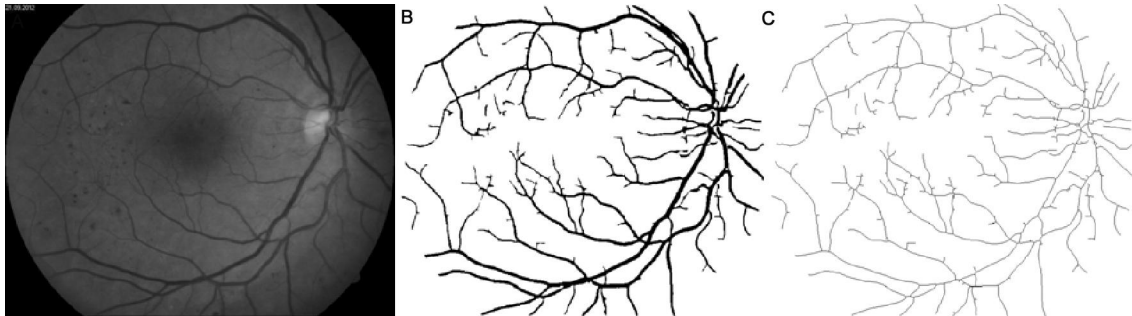


**Figure 2** Image of a mild NPDR with microaneurysms, dot hemorrhages and venous dilatation A: The grey image version; B: The segmented version; C: The skeletonized version.

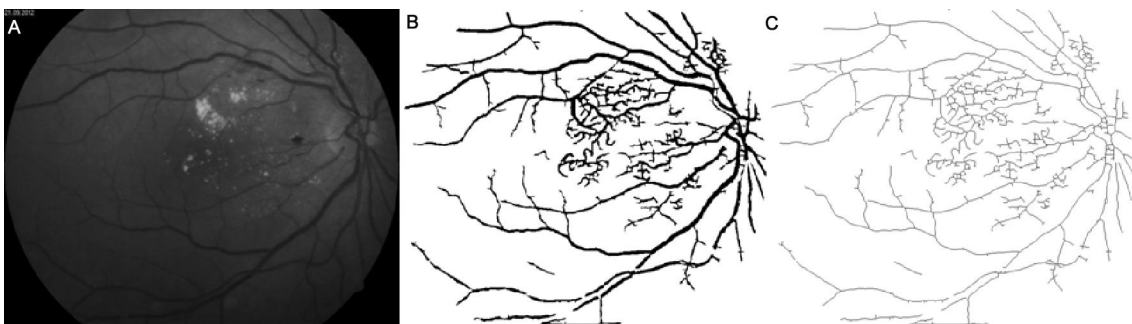


**Figure 3** Image of a moderate NPDR with circinate exudates, flame shaped and blotch hemorrhages and venous dilatation A: The grey image version; B: The segmented version; C: The skeletonized version.

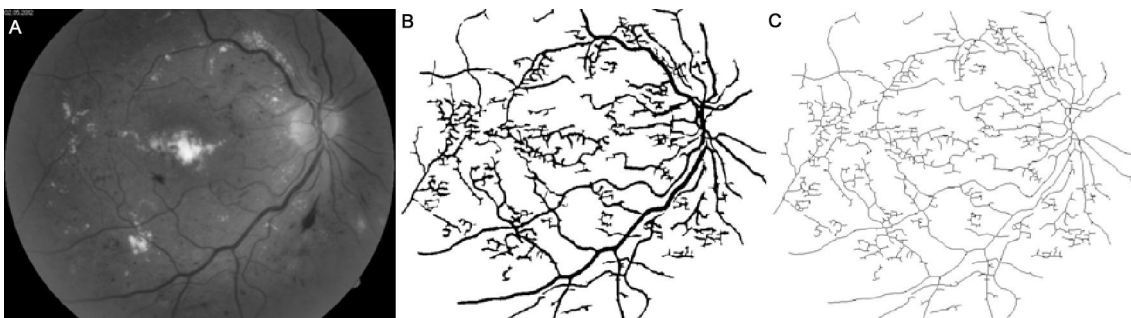


**Figure 4** Image of a severe NPDR with vascular bypasses, severe amounts of blotch hemorrhages, cotton wool spots and hard exudates presented in more than two quadrants of the retina A: The grey image version; B: The segmented version; C: The skeletonized version.

the skeletonized images were obtained with the ImageJ skeletonising algorithm.

In order to improve the understanding of the retinal microvascular architecture, fractal analysis was performed, for the entire retinal image, in two cases: a) on the segmented images (seg.) and b) on the skeletonized (skl.) version.

Fractal analysis was carried out using the ImageJ software

ver. 1.48g together with the FracLac plug-in ver 2.5, applying the standard box-counting algorithm to the digitized data.

The algorithm for fractal analysis was applied with the following options: a) grid positions - 30; b) calculating of grid calibers - use default box sizes. The range of box sizes used for the fractal dimension calculation was: 2 pixels (the minimum box size) and 45% from region of interest (the

maximum box size).

**Statistical Analysis** Microsoft Office Excel 2010 statistical functions were used to determine (mean±SD) of the fractal dimensions  $D$  obtained with ImageJ software. The statistical processing of the results obtained with ImageJ software (Table 1) was done using GraphPad InStat software program, version 5.00. Normal distribution of variables was previously assessed by means of the Kolmogorov-Smirnov test. It was found that fractal dimensions of the vascular trees followed a normal distribution. An analysis of variance (ANOVA) followed by post-hoc Scheffé comparison was performed to see whether significant differences were found between different diseased states. A value of  $P < 0.05$  was regarded as being statistically significant. The average results were expressed as mean value and SD.

**RESULTS**

For all analyzed cases (Table 1), the coefficients of correlation ( $R^2$ ) associated with fractal dimensions  $D$  were greater than 0.9945 representing a good linear correlation. An ( $R^2$ ) of 1.0 indicates that the regression line perfectly fits the data.

A summary of the obtained results of the fractal dimensions, all with mean±SD, of 172 analyzed images, for normal and DR status, in segmented and skeletonized variants is presented in the Table 1. Table 1 also shows that the mean values of the box-counting fractal dimensions were significantly different for normal and DR status.

In Figures 5-8 are shown the results of fractal analyses for retinal digital associated with Figures 1-4, in normal, segmented (seg.) and skeletonized (skl.) variants.

The average of fractal dimensions  $D$  for the normal images:  $D = 1.6232 \pm 0.0006$  (segmented version) and  $D = 1.5483 \pm 0.0004$  (skeletonized versions) is slightly lower than the corresponding values of mild NPDR images,  $D = 1.6253 \pm 0.0003$  (segmented version) and  $D = 1.5569 \pm 0.0005$  (skeletonized version).

The average of fractal dimensions  $D$  for the normal images (segmented and skeletonized versions) is higher than the corresponding values of moderate NPDR images,  $D = 1.6129 \pm 0.0006$  (segmented version) and  $D = 1.5437 \pm 0.0004$  (skeletonized version).

However, the average of fractal dimensions  $D$  for moderate NPDR images (segmented and skeletonized versions) is higher than the corresponding values of severe NPDR images,  $D = 1.5997 \pm 0.0005$  (segmented version) and  $D = 1.5391 \pm 0.0007$  (skeletonized version).

**DISCUSSION**

DR is a metabolic disorder of multiple aetiology [6]. Improvements in retinal imaging have led to quantification of architectural changes in the retinal vascular network of patients with DR. Our findings confirm that subtle changes in retinal microvascular network are influenced by DR and can be estimated using the fractal geometry. Also, the neovascularisation changes the branching patterns of the

**Table 1 The fractal dimensions of 172 analyzed images, for normal and DR status, in segmented and skeletonized variants  $\bar{x} \pm s$**

Status	Type	$D$	$P$
Normal	Seg.	1.6232±0.0006	0.011
	Skl.	1.5483±0.0004	0.012
Mild NPDR	Seg.	1.6253±0.0003	0.015
	Skl.	1.5569±0.0005	0.016
Moderate NPDR	Seg.	1.6129±0.0006	0.018
	Skl.	1.5437±0.0004	0.010
Severe NPDR	Seg.	1.5997±0.0005	0.021
	Skl.	1.5391±0.0007	0.018

retina vascular network, aspect highlighted in the different fractal dimensions between sub-groups.

Results in the present study are consistent with the argument that retinal microvasculature network is fractal because the vascular patterns are statistically self-similar over a range of length scales, the most common test for fractal structure [15].

The fractal results are absolutely determined by the density of the blood vessels [12,23,28]. For example, fundus images are of relatively low resolution compared to fluorescein angiography (FA) and potentially other more modern techniques. The many fractal smaller vessels detected by FA are not detected by fundus-based analysis [23]. In this study, the fundus images are of low resolution, but are clinically practical for current practice of global medicine.

Avakian *et al* [23] found that the region-based fractal analysis suggested that vessel density decreased in the NPDR macula relative to the normal macula and became relatively equivalent to vessel density in the normal and NPDR paramacular regions. Even at the relatively low imaging resolution of FA, the fractal dimension  $D$  may elucidate the significance of biological change during early stage disease in which space-filling dimensionality is of fundamental importance.

Cheng *et al* [28] found that retinal fundus photography has lower resolution to image smaller vessels compared with FA. Nevertheless, fundus photography is clinically more accessible and less invasive than FA. Also, it was demonstrated that, in older persons, these retinal vascular parameters, particularly tortuosity and caliber, are associated with diabetes and retinopathy signs, although the specific pattern of associations and the underlying mechanisms for these changes are different. Their findings highlight the usefulness of studying the retinal vasculature in gaining insights and clues into early and later pathways in diabetes and its microvascular manifestations.

This study confirms a part of the obtained results of fractal analysis determined by Cheung *et al* [28] concerning the relationship of DR with fractal dimensions in persons with diabetes: A) model 1: 1) no DR (level 10),  $D = 1.398$ ; 2) minimal DR (level 15),  $D = 1.408$ ; 3) mild DR (level 20 to 35),  $D = 1.41$ ; 4) moderate-to-severe DR (level  $\geq 43$ ),  $D = 1.385$  ( $P$  for trend equal with 0.057). B) model 2: 1) no DR

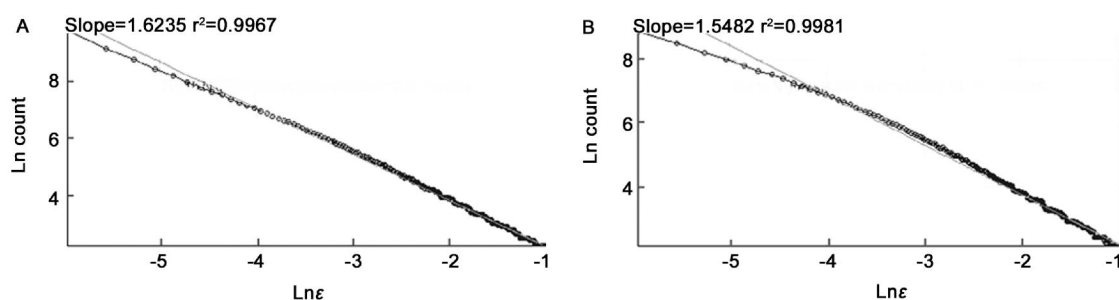


Figure 5 The Ln (count) versus Ln ( $\epsilon$ ) A: Segmented version; B: Skeletonized version.

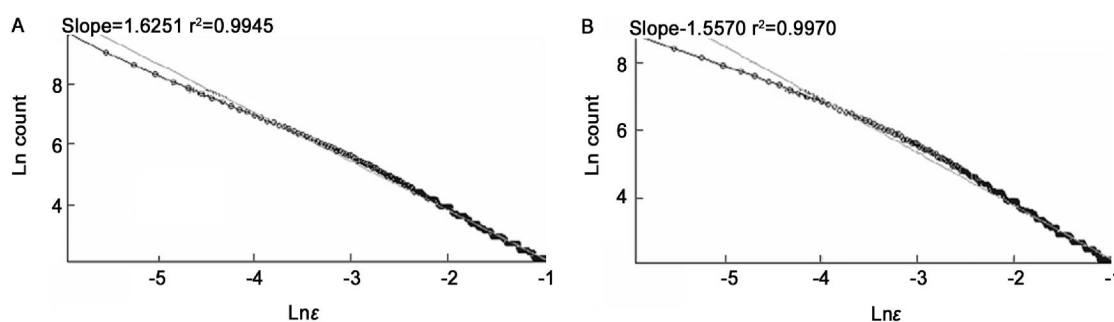


Figure 6 The Ln (count) versus Ln ( $\epsilon$ ) A: Segmented version; B: Skeletonized version.

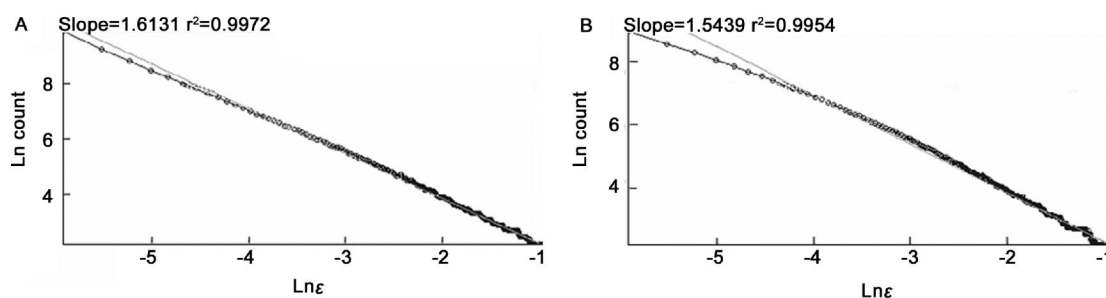


Figure 7 The Ln (count) versus Ln ( $\epsilon$ ) A: Segmented version; B: Skeletonized version.

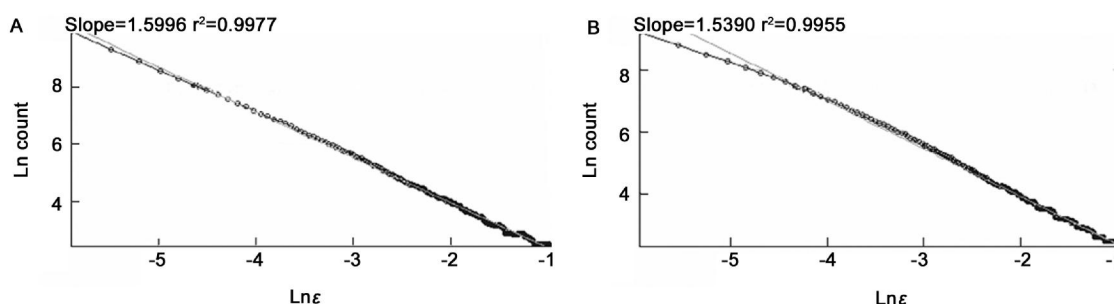


Figure 8 The Ln (count) versus Ln ( $\epsilon$ ) A: Segmented version; B: Skeletonized version.

(level 10),  $D=1.400$ ; 2) minimal DR (level 15),  $D=1.411$ ; 3) mild DR (level 20 to 35),  $D=1.413$ ; 4) moderate-to-severe DR (level  $\geq 43$ ),  $D=1.388$  ( $P$  for trend equal with 0.092).

In conclusion, the retinal vasculature is arranged in a three-dimensional network that can be directly visualized and monitored repeatedly over time. The effects of diabetes on the pattern and architecture of the retinal microvasculature are of great importance to a more complete understanding of the early and basic pathophysiological mechanisms of DR. The obtained results showed that the fractal analysis is a useful tool to be used in order to distinguish differences in the retinal vascular network geometry of patients with DR from healthy individuals.

## ACKNOWLEDGEMENTS

**Conflicts of Interest:** Tălu S, None; Călugăru DM, None; Lupascu CA, None.

## REFERENCES

- 1 Patton N, Aslam TM, MacGillivray T, Deary IJ, Dhillon B, Eikelboom RH, Yogesana K, Constable IJ. Retinal image analysis: concepts, applications and potential. *Prog Retin Eye Res* 2006;25(1):99-127
- 2 Jousseaume AM, Gardner TW, Kirchhof B, Ryan SJ (Eds.). *Retinal Vascular Disease* Germany:Springer;2007
- 3 Holz FG, Spaide RF (Eds.). *Medical Retina. Focus on Retinal Imaging* Germany:Springer;2010:8-9
- 4 Tălu S, Tălu M, Giovanzana S, Shah R. The history and use of optical coherence tomography in ophthalmology. *HVM Bioflux* 2011;3(1):29-32
- 5 Tălu S. Mathematical models of human retina. *Oftalmologia* 2011;55(3):

74–81

6 Browning DJ (Ed.). *Diabetic Retinopathy: Evidence-Based Management* USA:Springer;2010

7 Cunha-Vaz J. *Diabetic Retinopathy*. Singapore: World Scientific Publishing Co. Pte. Ltd.;2011

8 Tălu SD. *Ophthalmologie – Cours Cluj-Napoca, Romania: Medical publishing house “Iuliu Hatieganu”*;2005

9 Yam JC, Kwok AK. *Update on the treatment of diabetic retinopathy. Hong Kong Med J* 2007;13(1):46–60

10 Teng T, Lefley M, Claremont D. Progress towards automated diabetic ocular screening: a review of image analysis and intelligent systems for diabetic retinopathy. *Med Biol Eng Comput* 2002;40(1):2–13

11 Wilkinson CP, Ferris FL 3rd, Klein RE, Lee PP, Agardh CD, Davis M, Dills D, Kambik A, Pararajasegaram R, Verdaguer JT; Global Diabetic Retinopathy Project Group. Proposed international clinical diabetic retinopathy and diabetic macular edema disease severity scales. *Ophthalmology* 2003;110(9):1677–1682

12 Parsons-Wingter P, Radhakrishnan K, Vickerman MB, Kaiser PK. Oscillation of angiogenesis with vascular dropout in diabetic retinopathy by VESSEL GENERATION analysis (VESGEN). *Invest Ophthalmol Vis Sci* 2010;51(1):498–507

13 Kyriacos S, Nekka F, Vicco P, Cartilier L. The retinal vasculature: towards an understanding of the formation process. In: Vehel LJ, Lutton E, Tricot G (Eds.). *Fractals in Engineering: From Theory to Industrial Applications* Germany:Springer;1997:383–397

14 Szabo B, Tălu S, Lupascu CA. Application of fractal dimension in analysis of human retinal images in malignant choroidal melanoma patients. *Sylvan Journal* 2014;158(7):1–10

15 Tălu S, Giovanzana S. Fractal and multifractal analysis of human retinal vascular network: a review. *HVM Bioflux* 2011;3(3):205–212

16 Tălu S. Characterization of retinal vessel networks in human retinal imagery using quantitative descriptors. *HVM Bioflux* 2013;5(2):52–57

17 Tălu S. Fractal analysis of normal retinal vascular network. *Oftalmologia* 2011;55(4):11–16

18 Tălu S, Giovanzana S. Image analysis of the normal human retinal vasculature using fractal geometry. *HVM Bioflux* 2012;4(1):14–18

19 Azemin MZ, Kumar DK, Wong TY, Wang JJ, Mitchell P, Kawasaki R, Wu H. Age-related rarefaction in the fractal dimension of retinal vessel. *Neurobiol Aging* 2012;33(1):194.e1–4

20 Tălu S. Multifractal characterization of human retinal blood vessels. *Oftalmologia* 2012;56(2):63–71

21 Tălu S. Multifractal geometry in analysis and processing of digital retinal photographs for early diagnosis of human diabetic macular edema. *Curr Eye Res* 2013;38(7):781–792

22 Tălu S, Stach S, Sueiras V, Ziebarth NM. Fractal analysis of AFM images of the surface of Bowman's membrane of the human cornea. *Ann Biomed Eng* 2015;43(4):906–916

23 Avakian A, Kalina RE, Sage EH, Rambhia AH, Elliott KE, Chuang EL, Clark JI, Hwang JN, Parsons-Wingter P. Fractal analysis of region-based vascular change in the normal and non-proliferative diabetic retina. *Curr Eye Res* 2002;24(4):274–280

24 Lim SW, Cheung N, Wang JJ, Donaghue KC, Liew G, Islam FM, Jenkins AJ, Wong TY. Retinal vascular fractal dimension and risk of early diabetic retinopathy: a prospective study of children and adolescents with type 1

diabetes. *Diabetes Care* 2009;32(11):2081–2083

25 Cheung N, Donaghue KC, Liew G, Rogers SL, Wang JJ, Lim SW, Jenkins AJ, Hsu W, Li Lee M, Wong TY. Quantitative assessment of early diabetic retinopathy using fractal analysis. *Diabetes Care* 2009;32(1):106–110

26 Kunicki AC, Oliveira AJ, Mendonca MB, Barbosa CT, Nogueira RA. Can the fractal dimension be applied for the early diagnosis of non-proliferative diabetic retinopathy? *Braz J Med Biol Res* 2009;42(10):930–934

27 Grauslund J, Green A, Kawasaki R, Hodgson L, Sjolie AK, Wong TY. Retinal vascular fractals and microvascular and macrovascular complications in type 1 diabetes. *Ophthalmology* 2010;117(7):1400–1405

28 Cheung CY, Lamoureux E, Ikram MK, Sasongko MB, Ding J, Zheng Y, Mitchell P, Wang JJ, Wong TY. Retinal vascular geometry in Asian persons with diabetes and retinopathy. *J Diabetes Sci Technol* 2012;6(3):595–605

29 Yau JW, Kawasaki R, Islam FM, Shaw J, Zimmet P, Wang JJ, Wong TY. Retinal fractal dimension is increased in persons with diabetes but not impaired glucose metabolism: the Australian Diabetes, Obesity and Lifestyle (AusDiab) study. *Diabetologia* 2010;53(9):2042–2045

30 Nagaoka T, Yoshida A. Relationship between retinal fractal dimensions and retinal circulation in patients with type 2 diabetes mellitus. *Curr Eye Res* 2013;38(11):1148–1152

31 Stosic T, Stosic BD. Multifractal analysis of human retinal vessels. *IEEE Trans Med Imaging* 2006;25(8):1101–1107

32 Khan MI, Shaikh H, Mansuri AM, Soni P. A review of retinal vessel segmentation techniques and algorithms. *Int J Computer Technology and Applications* 2011;2(5):1140–1144

33 Tălu S. Mathematical methods used in monofractal and multifractal analysis for the processing of biological and medical data and images. *ABAH Bioflux* 2012;4(1):1–4

34 Tălu S. Texture analysis methods for the characterisation of biological and medical images. *ETBA Bioflux* 2012;4(1):8–12

35 Tălu S. The influence of the retinal blood vessels segmentation algorithm on the monofractal. *Oftalmologia* 2012;56(3):73–83

36 Tălu S, Vlăduțiu C, Popescu LA, Lupascu CA, Vesa SC, Tălu SD. Fractal and lacunarity analysis of human retinal vessel arborisation in normal and amblyopic eyes. *HVM Bioflux* 2013;5(2):45–51

37 Falconer K. *Fractal Geometry: Mathematical Foundations and Applications* 2nd Edition. UK: John Wiley & Sons Ltd;2003

38 Lupascu CA, Tegolo D. Stable automatic unsupervised segmentation of retinal vessels using Self-organizing Maps and a modified Fuzzy C-Means clustering. *Fuzzy Logic and Applications*. Trani, Italy;2011:244–252

39 Lupascu CA, Tegolo D, Trucco E. FABC: retinal vessel segmentation using AdaBoost. *IEEE Trans Inf Technol Biomed* 2010;14(5):1267–1274

40 Lupascu CA, Tegolo D. Automatic unsupervised segmentation of retinal vessels using self-organizing maps and K-means clustering. Proc. of CIBB 2010, Palermo, Italy;2010:263–274

41 Lupascu CA, Tegolo D, Trucco E. A comparative study on feature selection for retinal vessel segmentation using FABC. *Computer Analysis of Images and Patterns*. Germany:Springer Berlin Heidelberg;2009:655–662

42 Gould DJ, Vadakkan TJ, Poché RA, Dickinson ME. Multifractal and lacunarity analysis of microvascular morphology and remodeling. *Microcirculation* 2011;18(2):136–151